Hyperfine Interact
DOI 10.1007/s10751-013-0968-5

Mössbauer spectroscopy for optimising systems for environmental remediation

R. L. Fletcher-Wood · C. Gorin · S. D. Forder · P. A. Bingham · J. A. Hriljac

Abstract Mössbauer spectroscopy was used to examine Fe-containing microporous materials zeolite X and AlPO-5 designed for the reduction of Cr(VI) to Cr(III) and Cr(III) uptake. XRD, XRF, EPR and XPS were used to provide supporting information. AlPO-5 was found to only incorporate inactive Fe(III), whilst Fe(II) and Fe(III) were identified in zeolite X across a distribution of sites. Fe coordinates to oxygen atoms belonging to both water molecules and framework positions. EPR confirmed these findings and showed how the site distribution narrows upon dehydration. XPS showed that a distribution of Fe sites exists at the sample surface. Mössbauer spectroscopy was also used to track oxidation and reduction processes in Fe-zeolite X. Over time, gradual Fe oxidation takes place in air-exposed samples. Reduction under hydrogen flow increases the populations of low oxidation state Fe; as the reaction time increases, Fe(II) populations first increase, then decrease as Fe(0) is evolved.

Keywords Mössbauer · Zeolite · AlPO · Microporous · Chromium · Remediation

1 Introduction

Widespread use of chromium in industry has led to concern over safe disposal of carcinogenic Cr(VI) waste. Due to its many applications, there is no universal replacement for chromium and its substitution is therefore gradual and expensive. As such, the industrial demand for chromium persists.

Proceedings of the 32nd International Conference on the Applications of the Mössbauer Effect (ICAME 2013) held in Opatija, Croatia, 1–6 September 2013

R. L. Fletcher-Wood · J. A. Hriljac (✉)
School of Chemistry, The University of Birmingham, Birmingham B15 2TT, UK
e-mail: j.a.hriljac@bham.ac.uk

C. Gorin · S. D. Forder · P. A. Bingham
Materials and Engineering Research Institute, Sheffield Hallam University, Sheffield S1 1WB, UK

Published online: 26 November 2013

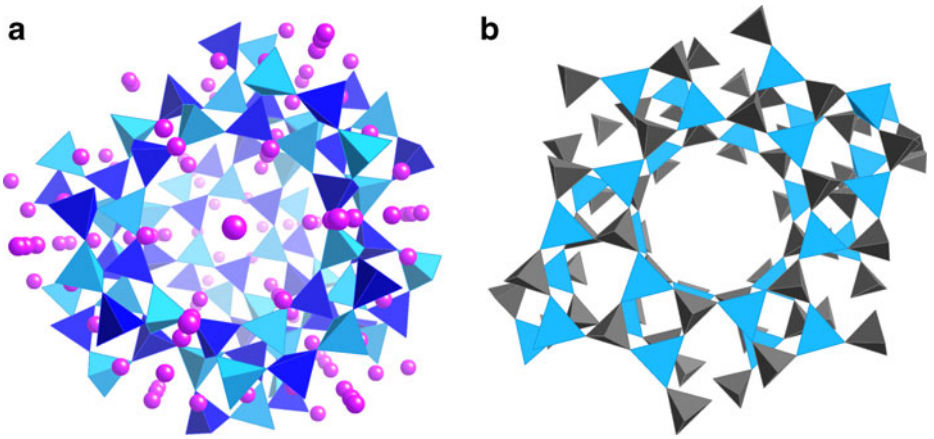

Fig. 1 Structures of **a** zeolite X with intercalated metal ions and **b** AlPO-5

Cr(VI) exists in waste waters as chromate or dichromate, depending on pH, such that it can only be taken up by anion adsorbers, for which there exists limited scope, since many are not stable under reaction conditions. The majority of existing Cr(VI) treatments involve chemical reduction to Cr(III) and precipitation of its hydroxides which, since Cr is not readily extracted, are then dumped as solid waste.

Microporous solids containing oxidisable charge-balancing cations have been proposed as materials to remove and recycle chromium from waste water via initial reduction of (di)chromate to cationic hydrated Cr(III) species and subsequent selective adsorption of these [1]. Fe(II) and Mn(II) drive the reduction (1).

$$\begin{aligned} 3{Fe^{2+}}_{(s)} + {Cr^{6+}}_{(aq)} &\rightarrow 2{Fe^{3+}}_{(aq)} + {Cr^{3+}}_{(s)} + {Fe^{3+}}_{(s)} \\ 3{Mn^{2+}}_{(s)} + 2{Cr^{6+}}_{(aq)} &\rightarrow 3{Mn^{4+}}_{(aq)} + 2{Cr^{3+}}_{(s)} \end{aligned} \quad (1)$$

Equation (1) proposed mechanism for Cr(VI) reduction and uptake into microporous solids by redox-active charge-balancing cations

Two types of microporous solids that act as molecular sieves are zeolites and aluminium phosphates (AlPOs). Zeolites (Fig. 1a) consist of complete corner-sharing SiO_4 and AlO_4 tetrahedra and are characterized by a O/(Al+Si) ratio of 2:1. Si tetrahedra are electronically neutral, whilst the 3+ valency of Al gives rise to a −1 charge per Al, producing a three-dimensional anionic framework compensated for by cations resting in the pore cavities of the structure [2]. AlPOs (Fig. 1b) have an analogous "zeotype" structure, with Al(III) and P(V) tetrahedra in a 1:1 ratio. These frameworks are electrostatically neutral, but charged cations may be incorporated onto framework and extra-framework sites during initial synthesis to produce redox active centres [3, 4]. In this work we attempted to introduce some Fe(II) for Al(III) which would produce a negatively charged framework and a need for charge balancing cations inside the pores. Exact pore characteristics determine the specificity of a molecular sieve for its guest species. The results presented here focus on zeolite X and AlPO-5, which have 8 Å and 7.3 Å pore sizes respectively [5], large enough to contain the hydrated Cr(III) species of 4.61 Å diameter [6].

2 Experimental

Zeolite X was synthesised by combining two solutions: 5.69 g sodium aluminate and 1.23 g of NaOH in 116 ml deionised water, with 27.08 g sodium silicate and 1.23 g NaOH in 104 ml deionised water. The combined solution was shaken vigorously for one hour at room temperature and warmed in polypropylene bottles in a furnace at 90 °C for 20 h with periodic shaking for the first 3 h. The crystallised zeolites were then dried under suction filtration. Iron exchanges were performed after the initial synthesis. 2.5 g of zeolite was stirred with 3.45 g of green Fe(II)SO_4.7H_2O (a 3–4 fold excess) in 125 ml of water under nitrogen gas. After stirring overnight, the zeolite was filtered off and dried at room temperature under vacuum on the Schlenk line and later stored in a desiccator in an argon-filled glovebox. Gentle heating initiated a green to brown transition indicative of oxidation of Fe(II) to Fe(III). Some samples were reduced under continuous hydrogen gas flow from a 90:10 N_2:H_2 cylinder in a tube furnace heated to 500 °C. The furnace was allowed to cool to room temperature before samples were removed and stored in an argon-filled glovebox. The Fe-$AlPO_4$-5 was synthesised by a method adapted from Girnus et al. [7]. Iron(II) acetate was included in the synthesis, substituting for an equimolar amount of aluminium isopropoxide. After filtering and washing with water, the crystals were calcined in air at 600 °C overnight to remove the organic template. Calcined and uncalcined products were obtained.

0.5 g of one Fe-AlPO-5 and one Fe-zeolite X were each stirred with 25 ml of 0.02 M sodium dichromate solution before being allowed to stand overnight. The solids were filtered, washed and dried under suction filtration before analysis.

X-Ray Diffraction (XRD) was used to verify the structures of the synthesised materials. Routine measurements were collected on the Bruker D8 ADVANCE and D5005 powder diffractometers. Elemental quantification was carried out by X-Ray Fluorescence spectroscopy (XRF) on a Bruker S8 Tiger, with an S8 Collector and Spectra Plus Launcher software. Mössbauer spectroscopy was employed for the identification of ion oxidation states and local environments and compared with Electron Paramagnetic Resonance spectroscopy (EPR) and X-Ray Photoelectric Spectroscopy (XPS). EPR spectra were collected on a Bruker EMX EPR Spectrometer using BioSpin collection software and WinEPR analysis and XPS was collected at the Nexus Nanolab on a Thermo-Scientific K-Alpha. ^{57}Fe Mössbauer spectra were collected at room temperature on a Wissel constant acceleration spectrometer, using a ^{57}Co source in a rhodium matrix. Isomer shifts are relative to α-Fe. Air sensitive samples were sealed in the Mössbauer absorber discs mixed with graphite powder.

3 Results and discussion

3.1 Fe-AlPO-5

A small amount of Fe has been reported to incorporate into tetrahedral framework sites in some AlPOs, as observed by Mössbauer spectroscopy [8–10]. As-prepared hydrated Fe-AlPO-5 was inspected by Mössbauer spectroscopy both before and after ion exchange with chromium (VI) solution. The spectra were best fitted with one Lorentzian doublet corresponding to high spin octahedral Fe(III) sites, in agreement with the as-synthesised sample of Zenonos et al. (Fig. 2, Table 1) [10]. Isomer Shift (IS) and Quadrupole Splitting (QS) values of 0.40 and 0.66 mm/s respectively did not vary with exposure to Cr(VI) solution. The isomer shift value is typical of octahedral environments, but the low level of distortion shown by the quadrupole splitting parameter demonstrates that Fe(III) is not in tetrahedral

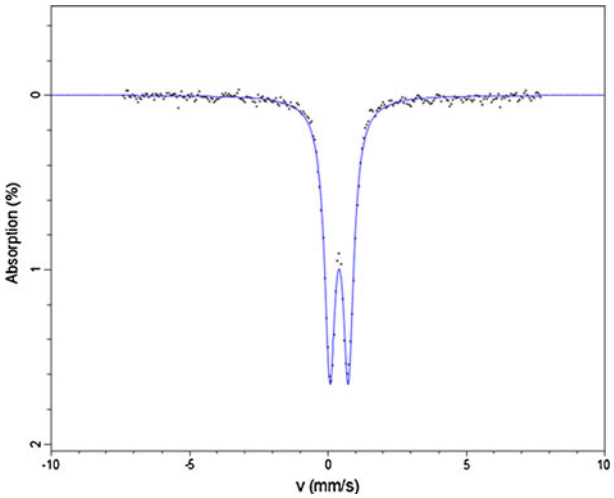

Fig. 2 Mössbauer spectrum of as-prepared hydrated Fe-AlPO-5 fitted with one Lorentzian doublet

framework positions. Narrower linewidths of 0.23 mm/s suggest that Fe(III) exists in similar sites throughout the material, coordinated to water molecules and resting within the AlPO pores. No Fe(II) was detected, implying complete oxidation in this system, making it inactive in the intended reaction. Unsurprisingly, there was no significant change to the system upon Cr exchange with an uptake of < 0.5 % Cr by mole %. This level of uptake is due to surface fouling.

3.2 Air-exposed Fe-zeolite X

The spectrum of air-exposed hydrated Fe-containing zeolite X was best fitted with two Lorentzian doublets (Fig. 3, Table 1). These are identified as high spin octahedral sites, belonging to Fe(III) and Fe(II). Unlike some studies of Fe(III) introduction to zeolites, all iron is extra framework since it was introduced post-synthesis [11].

The Fe(II) doublet is broad, with a linewidth of 0.45 mm/s. This supports a greater distribution of coordination environments than for Fe(III). Each Fe coordinates to six oxygen atoms from both framework positions and interstitial water molecules. The more flexible Fe-O_{water} bonds lend greater distortion and thus larger quadrupole splitting parameters. In a detailed study of Fe-zeolite Y, Garten et al. found that linewidths did not vary as a function of temperature and concluded a similar distribution of Fe environments in the hydrated zeolite [12].

These conclusions are supported by EPR data. A number of sites are visible in the spectrum of air-exposed hydrated Fe-zeolite X (Fig. 4), although Fe(II) is not evidenced, possibly due to low site population. The signal at $g = 2$ is commonly attributed to Fe(III) clusters undergoing exchange interactions, whilst the sites around $g = 4.3$ evidence tetrahedral or octahedral Fe(III) with low-symmetry rhombic distortions [13]. Upon dehydration, these sites consolidate into two distinct environments ($g = 2$ and $g = 4.3$), indicating that the majority of rhombically distorted sites are due to coordination to oxygen atoms in water molecules free within the structures (Fig. 5).

Table 1 Data from the fit for the Mössbauer spectra of Fe-containing microporous materials Mössbauer parameters are ±0.02 mm/s with IS relative to $\alpha-$Fe and site populations ∼ ±5 %

Figure	Material	Doublet Species	IS (mm/s)	QS (mm/s)	w+ (mm/s)	Site population (%)
2	Fe-AlPO-5	HS oct Fe(III)	0.40	0.66	0.23	100
	Cr-exchanged Fe-AlPO-5	HS oct Fe(III)	0.40	0.66	0.23	100
3	Air-exposed hydrated	HS oct Fe(III)	0.38	0.74	0.29	86
	Fe-zeolite X (brown)	HS oct Fe(II)	1.09	2.44	0.45	14
7	Non-air-exposed	HS oct Fe(III)	0.40	0.75	0.28	86
	Fe-zeolite X (green)	HS oct Fe(II)	1.10	2.53	0.31	14
8	Air-exposed hydrated	HS oct Fe(III)	0.39	0.77	0.29	90
	Fe-zeolite X (brown)	HS oct Fe(II)	0.92	2.78	0.38*	10

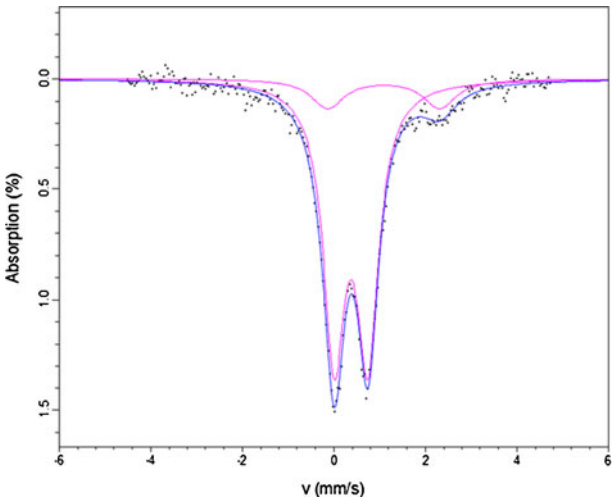

Fig. 3 Mössbauer spectrum of air-exposed hydrated Fe-containing zeolite X fitted with two Lorentzian doublets

Air-exposed hydrated Fe-zeolite X was also examined by XPS, a surface-sensitive technique. The XPS was not able to distinguish iron oxidation states, but broad peaks, as shown by the values for the FWHM, support a distribution of Fe sites (Fig. 6).

3.3 Gradual spontaneous oxidation of Fe-zeolite X

Fe-containing zeolites were observed to undergo a colour change upon exposure to air, indicating rapid aerial oxidation of surface species from green Fe(II) to brown Fe(III). However, Mössbauer spectroscopy discerns no change in relative Fe(II) and Fe(III) proportions between the as-prepared hydrated air-exposed and non-air-exposed samples (see Table 1). The non-air-exposed sample is likely to have a lower water content, since it is partially dried under vacuum and stored in a dry environment under argon gas.

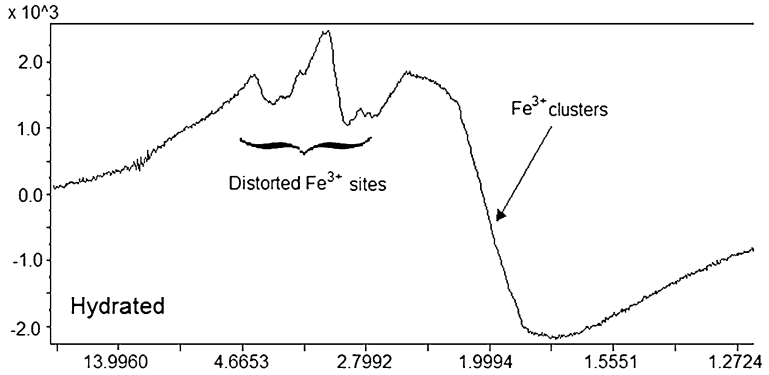

Fig. 4 EPR spectrum of air-exposed hydrated Fe-zeolite X with sites labelled and x-axis logarithmic g-factor

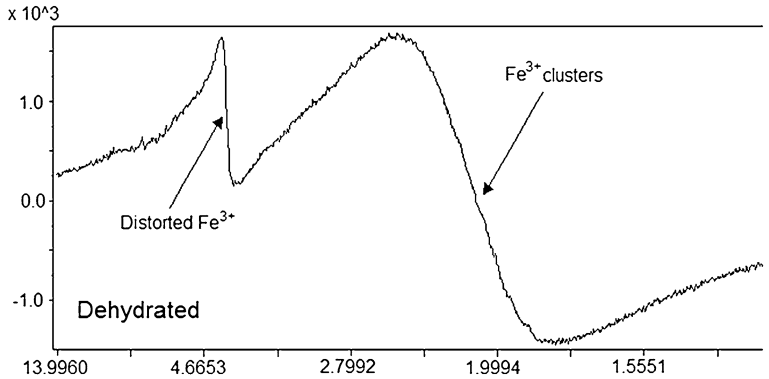

Fig. 5 EPR spectrum of air-exposed dehydrated Fe-zeolite X with sites labelled and x-axis logarithmic g-factor

Non-air-exposed Fe-zeolite X was fitted to two Lorentzian doublets for octahedral high spin iron sites (Fig. 7). Fe(III) parameters were very similar to those of the air-exposed sample, with IS of 0.40 mm/s, QS of 0.75 mm/s and linewidth of 0.28 mm/s. Fe(II) parameters differ slightly, with a higher quadrupole splitting (2.53 mm/s compared to 2.44 mm/s) and narrower linewidth (0.31 mm/s compared to 0.45 mm/s). Thus the lower level of hydration corresponds to a more distorted, more narrowly distributed coordination environment.

Gradual continuous oxidation taking place within air-exposed hydrated Fe-zeolite X may be observed by Mössbauer spectroscopy. This sample did not exhibit any further colour change. After 3 months of air exposure, the proportion of HS octahedral Fe(II) had decreased from 14 to 10 % (Fig. 8, Table 1). Fe(III) parameters remained similar to those obtained from the fit of the original spectrum (and are IS = 0.39 mm/s, QS = 0.77 mm/s), whilst a low IS of 0.92 mm/s and very high QS of 2.78 mm/s indicate a highly distorted octahedral environment for Fe(II). These parameters may have been affected by the fitting

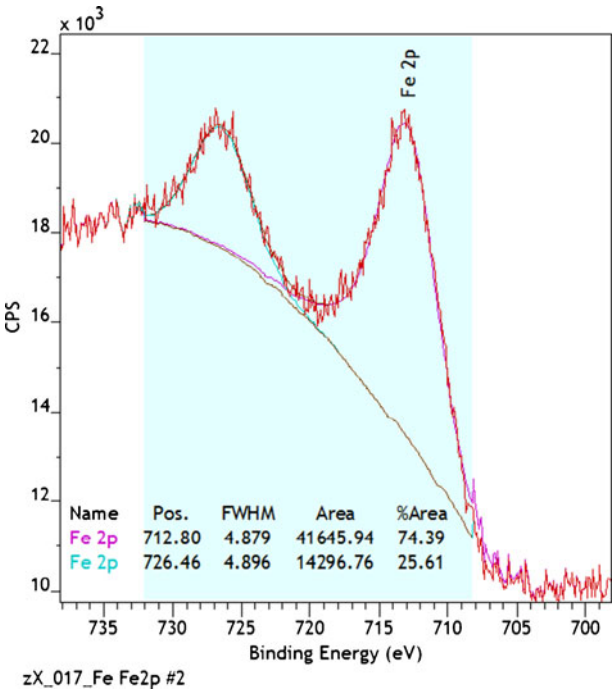

Fig. 6 XPS Fe 2p spectrum of air-exposed hydrated Fe-zeolite X

process, where the linewidth of Fe(II) was fixed at 0.38 mm/s. Left unfixed, the linewidth increases to over 1.40 mm/s giving conclusions which are not chemically sensible. This arises because of hyperfine splitting broadening [14, 15]. That this doesn't happen in the parent material suggests that iron may be migrating to the zeolite surface.

3.4 Reduced Fe-zeolite X

Low oxidation state Fe(II)-containing zeolite X or a system with Fe(0) particles are potential materials for Cr(VI) treatment. Reduction under hydrogen flow produces more low oxidation state iron to improve the extent of Cr(VI) reduction to Cr(III). Four samples were produced exposed to H_2 flow at 500 °C for 1, 3, 6 and 12 h to obtain increased Fe(II) populations and potentially Fe(0). These were compared with the parent material (0 h). Each spectrum was fitted to two Lorentzian doublets and parameters are listed in Table 2. Fe(0) was evolved at 3 h and fitted to a sextet. Across the series, the Fe(II) site population first increases, then decreases as Fe(0) is evolved, whilst the Fe(III) content continuously decreases. The other parameters do not vary significantly across the series (Table 2). The fact that magnetic ordering is seen for Fe(0) indicates particles must be forming that are at least on the order of 10 nm in size. These cannot form inside the normal zeolite framework, so could either be forming inside macropores due to structural degradation or migration onto the surface as has been seen before in other systems such as Pt-exchanged zeolite Y [16]. As there is no obvious degradation of the X-ray powder pattern it appears more likely that small particles are forming on the surface.

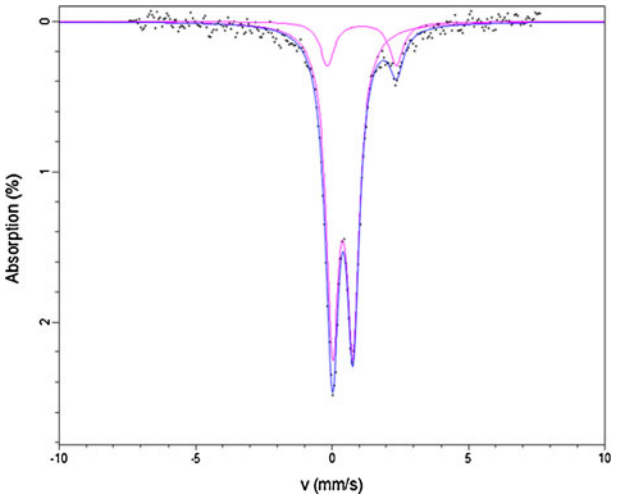

Fig. 7 Mössbauer spectrum of non-air-exposed Fe-zeolite X fitted with two Lorentzian doublets

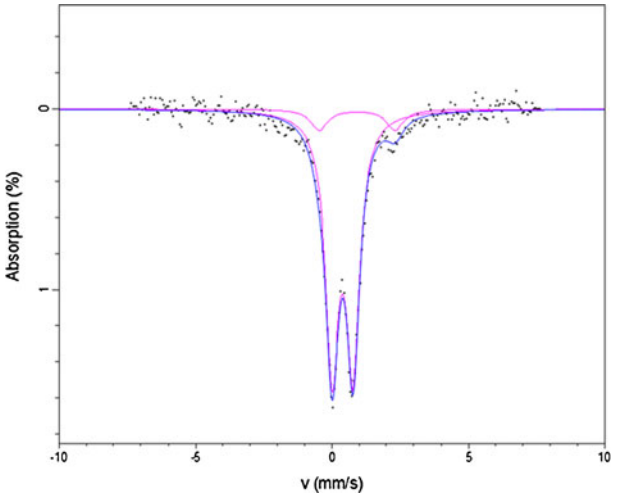

Fig. 8 Mössbauer spectrum of a 3-months air-exposed hydrated Fe-zeolite X fitted with two Lorentzian doublets

3.5 Cr-exchanged non-air-exposed Fe-zeolite X

As a proof of principle, Cr-exchange was carried out on non-air-exposed Fe-zeolite X. The Fe/Si molar ratio was calculated at 0.65 before Cr-exchange and 0.71 after Cr exchange. The Cr/Si molar ratio after exchange was 0.19 showing a significant uptake. XRF analysis confirmed the inclusion of chromium into the material, with accompanying loss of iron species. XPS data support our proposed mechanism: comparison to the National Institute of Standards and Technology (NIST) database, confirms that the chromium detected at the

Table 2 Data from the fit for the Mössbauer spectra of the hydrogen-reduced series of Fe-zeolite X Mössbauer parameters are ±0.02 mm/s with IS relative to α-Fe and site populations ∼ ±5 %

Sample	Doublet Species	IS (mm/s)	QS (mm/s)	w+ (mm/s)	Site (%)
0hrs	HS oct Fe(III)	0.37	0.84	0.28	93
	HS oct Fe(II)	1.22	2.26	0.18	7
1hr	HS oct Fe(III)	0.36	0.90	0.34	78
	HS oct Fe(II)	1.67	2.28	0.29	23
3hrs	HS oct Fe(III)	0.39	0.91	0.34	71
	HS oct Fe(II)	1.02	2.31	0.38	20
	Fe(0) sextet	0	B ∼ 33T	0.16	9
6hrs	HS oct Fe(III)	0.38	0.87	0.34	64
	HS oct Fe(II)	1.04	2.30	0.36	25
	Fe(0) sextet	0	B ∼ 33T	0.16	11
12 hrs	HS oct Fe(III)	0.37	0.87	0.32	60
	HS oct Fe(II)	1.04	2.25	0.38	13
	Fe(0) sextet	0	B ∼ 33T	0.14	27

sample surface is Cr(III), with a typical energy ∼586 eV. Cr(VI) has a higher oxidation state and thus binding energy ∼ 3 eV higher.

4 Summary

A distribution of iron sites exists throughout the zeolite samples studied here wherein Fe coordinates to oxygen atoms from both water molecules and framework positions. Dehydration to remove water gives a narrower distribution of coordination environments seen by EPR spectroscopy. A narrower distribution of Fe(III) sites was identified in AlPO-5, which cannot reduce Cr(VI) to Cr(III). XPS shows that the chromium taken up by Fe-zeolite X is Cr(III): that is, the intended reduction occurs at the sample surface, including loss of Fe species. However, XPS is a surface sensitive technique, and cannot conclude that ion exchanges occur inside the zeolite pores. Over time, gradual oxidation of Fe species takes place in air-exposed Fe-zeolite X. Reduction under hydrogen flow is introduced to increase the populations of low oxidation state Fe; as the reaction time increases, Fe(II) populations first increase, then decrease as Fe(0) particles are formed.

Acknowledgments We gratefully acknowledge Advantage West Midlands for XRD and XRF facilities, the School of Chemistry, University of Birmingham and EPSRC for funding and EPSRC for access to the Nexus XPS Facility at the University of Newcastle. We also thank Professor Frank Berry and Dr Simon Cotton for their assistance interpreting Mössbauer and EPR spectroscopies.

References

1. Lee, S., Lee, K., Park, J., Asce, M.: Simultaneous removal of Cd and CrVI using fe-loaded zeolite. J. Environ. Eng., 445–50 (2006)
2. Smart, L., Moore, E.A.: Zeolites and related structures. In: Solid State Chemistry: An Introduction, 3rd edn, pp. 300–345. Chapman & Hall (1995)

3. Subrahmanyam, C., Viswanathan, B., Varadarajan, T.K.: Synthesis, characterisation and catalytic activity of mesoporous trivalent iron substituted aluminophosphates. J. Molec. Cat. A Chem. **223**, 149–153 (2004)
4. Prakash, A.M., Hartmann, M., Zhu, Z., Kevan, L.: Incorporation of transition metal ions into MeAPO/MeAPSO molecular sieves. J. Phys. Chem. B **104**, 1610–1616 (2000)
5. Meier, W.M., Olson, D.H., Baerlocher, C.: Atlas of Zeolite Structure Types. Elsevier, London (1996)
6. Covarrubias, C., Garcı, R., Arriagada, R., Yanez, J., Garland, M.T.: Cr(III) exchange on zeolites obtained from kaolin and natural mordenite. Micro. Meso. Mater. **88**, 220–231 (2006)
7. Girnus, I., Jancke, K., Vetter, R., Richter-Mendau, J., Caro, J.: Large ALP04-5 crystals by microwave heating. Zeolites **15**, 33–39 (1995)
8. Das, J., Satyanaryana, C.V.V., Chakrabarty, D.K.: Substitution of Al in the AIPO-5 and AIPO-II Frameworks by Si and Fe: A study by mossbauer, magic-angle-spinning nuclear magnetic resonance and electron paramagnetic resonance spectroscopies and chemical probes. J. Chem. Soc. Faraday Trans. **88**(21), 3255–3261 (1992)
9. Cardile, C.M., Tapp, N.J., Milestone, N.B.: Synthesis and characterization of an iron-substituted aluminophosphate molecular sieve. Zeolites **10**(550), 90–94 (1990)
10. Zenonos, C., Sankar, G., Cor, F., Lewis, D.W., Pankhurst, Q., Catlow, C.R.: On the nature of iron species in iron substituted aluminophosphates. Phys. Chem. Chem. Phys. **4**(21), 5421–5429 (2002)
11. Awate, V.: Partial isomorphous substitution of Fe3+ in the LTL Framework. J. Phys. Chem. **97**, 9749–9753 (1993)
12. Garten, R.L., Deglass, W.N., Boudart, M.: A Mössbauer spectroscopic study of the reversible oxidation of ferrous ions in Y zeolite. J. Catal. **18**, 90–107 (1970)
13. Bingham, P., Parker, J.M., Searle, T., Williams, J.M., Smith, I.: Novel structural behaviour of iron in alkali alkaline-earth–silica glasses. Comptes Rendus Chimie **11**, 787–96 (2002)
14. Kurkjian, C.R.: Mössbauer spectroscopy in inorganic glasses. J. Non Cryst. Solids **3**, 157–194 (1970)
15. Williams, K.F.E., Johnson, C.E., Thomas, M.F.: Mössbauer spectroscopy measurement of iron oxidation states in float composition silica glasses. J. Non Cryst. Solids **226**, 19–23 (1998)
16. Pandya, K.I., Heald, S.M., Hriljac, J.A., Petrakis, L., Fraissard, J.: Characterization by EXAFS, NMR and other techniques of Pt/NaY zeolite at industrially relevant low concentrations of platinum. J. Phys. Chem. **100**, 5070–77 (1996)